Additive metallization of alumina with copper-titanium powder blends for power electronic applications

Christoph Hecht
Institute for Factory Automation and Production Systems
Friedrich-Alexander-Universität Erlangen-Nürnberg
Nuremberg, Germany
christoph.hecht@faps.fau.de

Eric Schadow
Institute for Factory Automation and Production Systems
Friedrich-Alexander-Universität Erlangen-Nürnberg
Nuremberg, Germany
eric.schadow@gmx.de

Mario Sprenger
Institute for Factory Automation and Production Systems
Friedrich-Alexander-Universität Erlangen-Nürnberg
Nuremberg, Germany
mario.sprenger@faps.fau.de

Felix Häußler
Institute for Factory Automation and Production Systems
Friedrich-Alexander-Universität Erlangen-Nürnberg
Nuremberg, Germany
felix.haeussler@faps.fau.de

Thomas Stoll
Professorship of Laser-based Additive Manufacturing
TUM School of Engineering and Design
Munich, Germany
thomas.stoll@tum.de

Jörg Franke
Institute for Factory Automation and Production Systems
Friedrich-Alexander-Universität Erlangen-Nürnberg
Erlangen, Germany
joerg.franke@faps.fau.de

***Abstract*— Additive manufacturing shows great potential to further increase the performance of power electronic modules through novel packaging concepts. Such an approach is the integrated manufacturing of metal-ceramic substrates by means of laser powder bed fusion of metals (PBF-LB/M). With this layered additive manufacturing process, planar ceramic substrates can be metallized and electrically functionalized for power electronic applications. In this paper Al_2O_3 ceramic substrates are metallized via PBF-LB/M by selectively melting applied powder layers with software defined geometries. The investigated powders are mixtures of copper and titanium powders with 1 wt.%, 5 wt.% and 10 wt.% titanium in order to enable bonding by creating a titanium-oxide reaction layer at the interface to the ceramic. Shear tests and microstructural investigations show that a subsequent heat treatment increases the adhesion and density of the metallization. By energy dispersive X-ray microscopy (EDX) the partial formation of reaction layers is detected.**

Keywords—Active Metal Brazing, Laser powder bed fusion, Power electronics, Substrates

I. INTRODUCTION

The increasing electrification of the entire energy and mobility sector, due to the existing climate change significantly caused by CO_2 emissions from the combustion of fossil fuels, is being driven forward with high priority in most industrialized countries. Only recently, it was decided within the EU that only CO_2 emission free engines will be permitted for the public motor vehicle sector from 2035 onwards [1] paving the way for electrically driven cars. For the industrial sector, greenhouse gas emissions can be reduced by up to 95 %, if a 60 % electrification rate is achieved [2]. In addition, the expansion of renewable energies such as solar and wind power also increasingly requires power electronic modules for the conversion of the electrical energy to match the requirements of electrical consumers like motors or heaters.

The presented work received funding from the Deutsche Forschungsgemeinschaft (DFG, German Research Foundation) – 434962551; 442921285.

A. Substrate technologies in power electronics packaging

Most commonly used as substrate materials in power electronic modules are metal-ceramic-interconnects due to an improved performance with regard to ampacity, insulation, thermal management and reliability characteristics compared to printed circuit boards based on organic materials. Such high power electronic substrates are commonly manufactured via two different processes:

- Direct Bonded Copper (DBC)
- Active Metal Brazing (AMB)

whereas AMB-substrates are more used for high performance applications with high requirements on thermo-mechanical stability and thermal conductivity. [3] Both technologies are described in the following:

The DBC-technology is based on an eutectic bonding of copper foils on alumina (Al_2O_3), zirconia toughened alumina (ZTA) or aluminum nitride (AlN) in a burning process in the range of 1065 °C and 1083 °C. At this temperature range, the eutectic of Cu_2O at the Cu-ceramic-interface forms a liquid wetting on the substrate [4]. The Cu-foils are either pre-oxidized or oxidized during the burning process in the furnance to form Cu_2O at the surface. With the wetting of the Cu_2O-eutectic on the ceramic, phases like $CuAl_2O_4$ (spinell) or $CuAlO_2$ (delafossit) are emerging that ensure a strong bonding between the two materials with a high bonding strength. [5] [6] [7]

The technology of Active Metal Brazing utilizes an active filler material to ensure a bonding between laminated copper foils and ceramic substrates. The filler material nowadays mostly contains a silver-based alloy with a share of 1 to 10 wt.% of reactive elements like titanium, hafnium or zirconium, that enable a wetting of the active solder (filler material) on the ceramic substrate [8]. Industrially used ceramic materials are mostly non-oxide ceramics like AlN or silicon nitride (Si_3N_4) due to the superior material properties with respect to mechanical strength and/or thermal conductivity. Nevertheless, both substrates are very

expensive compared to oxide-based ceramics, which makes substrate materials like Al_2O_3 interesting for future research and development concerning novel metallization techniques. The bonding mechanism is based on the emergence of a reaction zone between the ceramic substrate and the used active solder [9] whereas on the metal side (copper) an adequate wetting is given anyway, due to the lower surface energy of the metal, determined by the persistence of free electrons in the material. In the reaction zone between the active solder and the oxide-based ceramic different Magneli-phases, like Ti_3O_5, Ti_4O_7, TiO_2 [8] as well as $Ti_3Al[O]$-phases [10] are emerging that resist mechanical shear stresses of up to 180 MPa [11].

Nevertheless, both technologies have in common that they are exclusively used for planar metallization in the power electronic sector. Moreover, both methods require long process chains with different manufacturing steps like laminating, application of the active solder at AMB-substrates, burning, etching and cleaning with the usage of stencils and/or lithographic technologies. [3] Furthermore, according to the goal to apply sustainable technologies in the future, the usage of etching technologies shall be replaced with respect to ecological aspects. Additionally, just a horizontal integration of active and passive electronic elements for the power electronic device is possible, as the substrate itself is planar. As the power density of future power electronic devices needs to further increase to maintain or even reduce the spatial dimensions of the devices, a 3D- and additional vertical integration of electronic components will be necessary to keep up with the rising need for electric energy.

B. Additive Manufacturing: Laser Powder Bed Fusion

Generally, additive manufacturing processes are divided into seven categories, with powder bed fusion being the most important category for the material class of metals [12]. Layer by layer applied metal powder is melted with a beam source such as a laser or an electron beam. The schematic layout of a system for powder bed fusion of metals with a laser-based system (PBF-LB/M) is shown in Fig. 1.

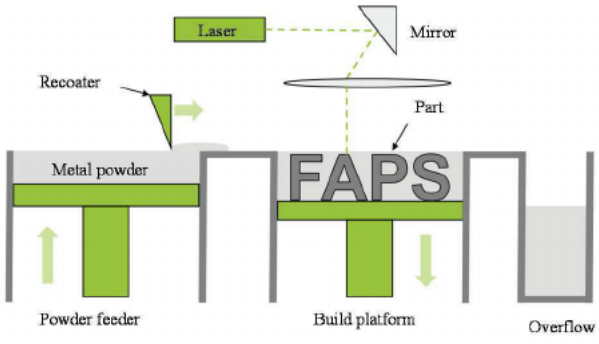

Fig. 1. Powder bed fusion of metals with a laser-based system (PBF-LB/M) [13].

Thin powder layers with a thickness between 20 and 100 micrometers are drawn from the powder reservoir onto the build platform with a recoater system. The layer is then irradiated with a finely focused laser according to the part cross-section and the build platform is lowered by one layer thickness. By building up a large number of layers, the component geometry is thus created, and all the unmelted powder can be reused after a sieving process. In the process, the parts are built up on a metallic build platform, so that subsequent separation is necessary. By replacing the metallic build platform with other substrates, metallizations can also be produced [13] as applied in this study to ceramic substrates. This way the ceramic can be functionalized for use in power electronic modules.

II. Machine and Materials

The investigations were performed on the PBF-LB/M-Machine Mlab Cusing R of the manufacturer Concept Laser, which is equipped with a fiber laser emitting at a wavelength of 1070 nm up to 500 W. The diameter of the laser spot on the build platform was set to 35 µm. In order to decrease the thermal shock during solidification and to enhance diffusion processes at the metal-ceramic interface, the building chamber was equipped with a heating module, which allowed preheating of the ceramic substrate to 300 °C. [14] The ceramic substrate was positioned in a milled pocket of an adapter plate, which was mounted onto the build platform. The residual oxygen in the argon flooded process chamber was held below 50 ppm, which was monitored with an Orbitalum ORBMax.

The processed powder was copper ETP of manufacturer Ecka Granules mixed with 1 wt.%, 5 wt.% and 10 wt.% titanium powder of manufacturer TLS Technik GmbH & Co. Spezialpulver KG. The copper powder is labeled with AK < 0.045 mm and has a particle size distribution of d_{10} = 11.60 µm and d_{90} = 42.85 µm. [15] The titanium powder is characterized with a d_{10} of 10 µm and a d_{90} of 45 µm according to the data sheet. Both powders have a spherical shape as shown in Fig. 2. The blending process was performed manually and with a vibratory plate for at least 30 minutes. The metallized substrates were 40x40x1 mm^3 Rubalit 708S plates of manufacturer CeramTec. Shear testing was conducted based on DIN EN 15340 with a XYZTEC Condor 150-3, which can apply a maximal shear force of 400 N. For subsequent thermal treatments, the tube furnance Gero Carbolite GHA 12/300 was flooded with argon 5.0 to reach a residual oxygen content of less than 10 ppm in the tube to avoid oxidation of the metallizations.

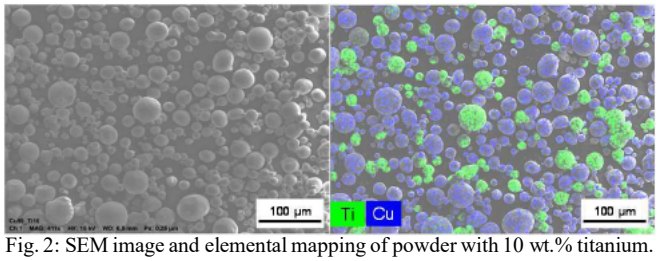

Fig. 2: SEM image and elemental mapping of powder with 10 wt.% titanium.

III. Metallizations with Varying Titanium Content

Due to the high affinity of titanium to react with oxygen, an influence of the titanium content in the metal powder mixture on the adhesive strength of the metallization on the Al_2O_3 ceramic is expected. This aspect will be investigated within this study.

A. Experimental design

Metallization studies were conducted according to Table I. For each parameter combination one cuboid metallization with a quadratic base of 5 mm edge length and a height of

360 µm was printed, which results from 12 layers of 30 µm thickness. In total 450 cubes on 51 ceramics were printed as one ceramic was metallized with up to 9 cubes. The samples were built up with an island exposure strategy, dividing the 5x5 mm^2 cross-section of the cuboids in the exposure plane into 25 1x1 mm^2 squares. In order to improve the powder deposition of the first layer, thin shims were placed between the build platform and the adapter plate.

TABLE I. Full factorial experimental design.

Parameter	Min.	Max.	Increment
Power in Watt	30	40	2
Scan speed in mm/s	550	750	50
Hatch in µm	10.5	24.5	3.5
Ti share in wt.%	1, 5, 10		

B. *Adhesion*

All samples within the experimental design according to Table I were subjected to shear testing. With a maximum load cell force of 400 N and a specimen cross-section of 25 mm^2, a maximal adhesive strength of 16 MPa can be obtained. The boxplot in Fig. 3 shows the results of the shear tests.

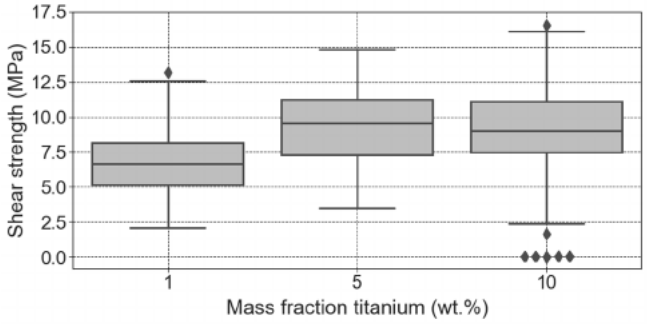

Fig. 3. Adhesion box plots of powder mixtures obtained by shear testing.

With an one-way analysis of variances (ANOVA) the obtained differences in mean adhesive strength between the different titanium shares are checked for statistical significance at a level of significance of 5 %. The mean value of the samples with 1 wt.% titanium differs significantly from the samples with 5 wt.% and 10 wt.% titanium. Between 5 wt.% and 10 wt.% no significant difference between the mean values of adhesion are obtained. So, the increase of titanium within the powder system improves the adhesion only within the range of 1 wt.% to 5 wt.% The mean values for all powder mixtures are depicted in Fig. 4.

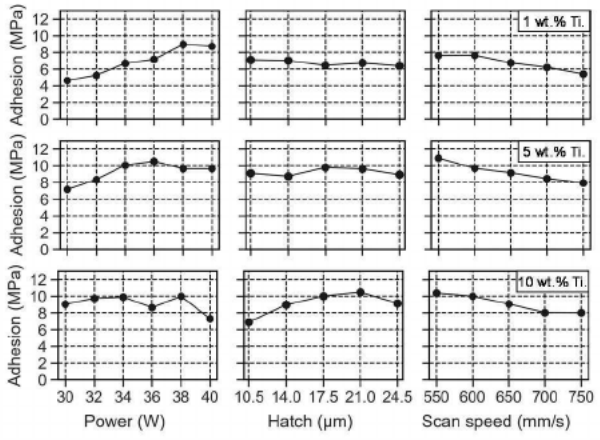

Fig. 4. Mean adhesion at factor levels according to the experimental design: 1 wt.% titanium (top), 5 wt.% titanium (middle), 10 wt.% titanium (bottom).

At 1 wt.% the laser power and scan speed have a strong impact on the adhesion in such a way, that higher laser powers and lower scan speeds result in stronger adhesion. At varying hatches, the adhesion alters only slightly within less than 1 MPa. Therefore, within the considered experimental design the adhesion improves with increasing energy input. For each parameter, the highest mean value is obtained for parameter range limiting values and therefore no optimal parameters are obtained. For 5 wt.% titanium, a laser power of 34 W and 36 W results in samples with a mean adhesion of more than 10 MPa. Similar to 1 wt.% the hatch has less impact on the adhesion. The strongest bonding is obtained at 550 mm/s. This applies also to powders with 10 wt.% titanium. In contrast to 1 wt.% and 5 wt.%, the hatch has a strong impact and the laser power less impact at 10 wt.% titanium. Adhesion maximizing parameters within the investigated parameter range are calculated based on a regression model. The result can be obtained from Table II. The increasing laser power with decreasing share of titanium can be subjected to the high reflectivity of copper as more power is required for fusion. With regard to the scan speed, strongest adhesion is obtained at 550 mm/s. At lower scan speed, the material maintains longer in the molten state and diffusion processes are enhanced. Due to the high adhesive strength and low titanium content, metallizations with 5 wt.% titanium will be further investigated in heat treatment studies. To check the reproducibility of the identified process parameters for 5 wt.% titanium given in Table IV, a control group of 27 pads on three different ceramics is manufactured and sheared off. Due to machine limitation, the laser power was rounded to an integer value of 38 W. The obtained mean adhesion of 15.2 MPa is even higher than the model prediction of 13.2 MPa. The obtained standard deviation is 2.6 MPa.

TABLE II. Adhesion maximizing parameters.

Parameter	Share of titanium in wt.%			Unit
	1	5	10	
Power	40	38.7	31.5	Watt
Scan speed	550	550	550	mm/s
Hatch	10.5	24.5	16.7	µm
Predicted adhesion of regression model	10.1	13.2	13.2	MPa

IV. HEAT TREATMENT

Subsequent heat treatments according to Table III are performed on samples with 5 wt.%. The edge length of the quadratic base area was reduced from 5 mm to 3 mm in order to allow measurements up to 44.4 MPa with the load cell of the shear testing equipment, which is limited to a shear force of 400 N.

TABLE III. Experimental design for heat treatment.

Parameter	Heat treatment		
	1	2	3
Peak temperatur in °C	850	850	950
Dwell time at peak temperature in minutes	5	60	60

A. *Cross-section analysis*

The effect of the heat treatment on the metallization can be observed in cross-section analysis shown inFig. 5. The relative

density increases according to Table IV. The values are obtained by evaluating the share of white and black pixels after conversion to a binary image.

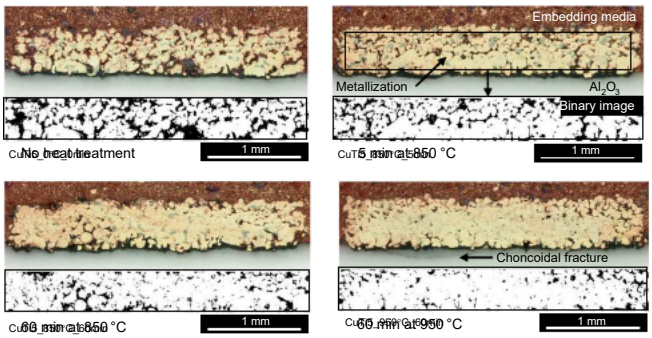

Fig. 5. Cross-section incident light micrographs of heat-treated samples and associated binary images for relative density measurements.

This increase in relative density can be subjected to time and temperature dependent solid-state diffusion processes, which intensify at high temperatures. [16] At 950 °C conchoidal fractures in the ceramic occur, which are a consequence of thermo-mechanical stresses in brittle materials like Al_2O_3. [17]

TABLE IV. Relativ densities obtained by optical measurement.

Treatment	Relative density in %
No treatment	72.2
1	82.4
2	87.1
3	93.8

B. *Shear tests*

The reduction of the base area of the metallization to 9 mm^2 allows to measure adhesion up to 44.4 MPa. For each heat treatment 12 samples on one ceramic are manufactured and shear tested. The resulting box plots are shown in Fig. 6. By decreasing the base area of the metallization, stronger adhesion is obtained as the mean adhesion increases by 3 MPa to 18.2 MPa in the as printed state in comparison to the control group in section 3B with a quadric base of 5 mm edge length. With increasing dwell times and temperatures, the mean adhesion improves to 20.8 MPa, 22.8 MPa and 27.8 MPa. At 950 °C the adhesion fluctuates more strongly as shown in the box plot in Fig. 6. This can be subjected to conchoidal fractures in the ceramic interface, which are observed in cross-section analysis in Fig. 5.

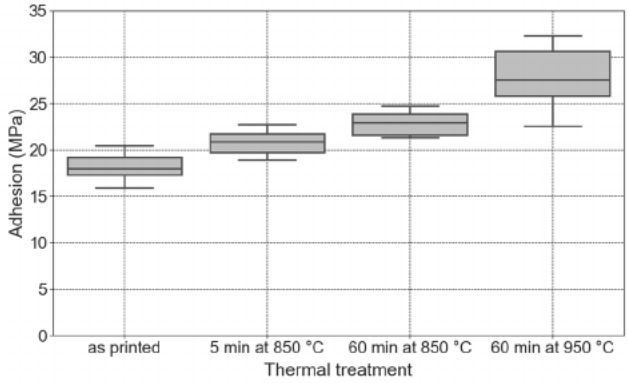

Fig. 6. Adhesion box plots of heat-treated samples with 5 wt.% titanium.

C. *Microstructure*

The impact of the heat treatment on the microstructure was further analyzed via EDX analysis. The elemental mapping of O, Cu and Ti at the cross-section is shown in Fig. 7. The element distribution of the sample without heat treat shows that no homogeneous alloying by the laser process is obtained, because undissolved titanium particles are embedded in the copper matrix.

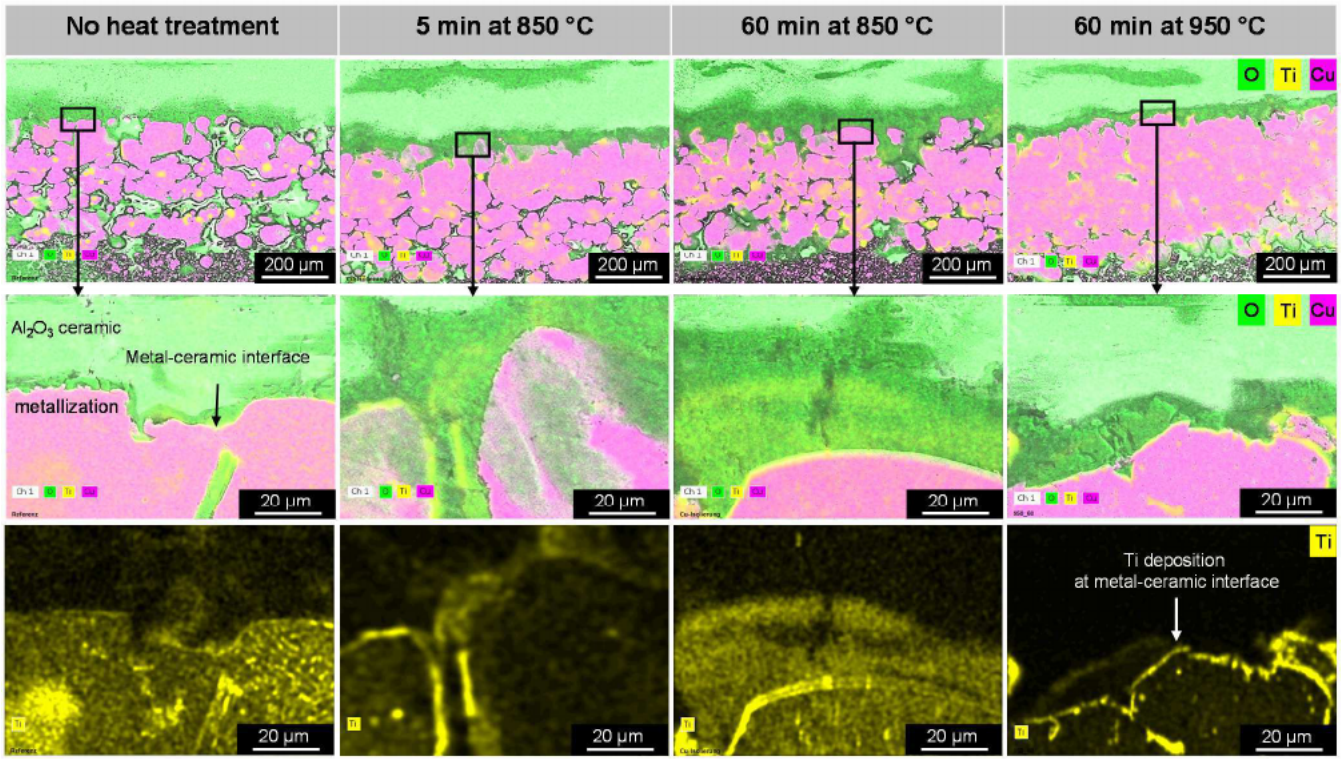

Fig. 7. Elemental mapping of O, Cu and Ti at cross-section after heat treatment of specimen with 5 wt.% titanium.

TABLE V. Elemental composition at positions according to Fig. 8.

Element	Elemental composition in at.%								
	Position							Mean	Std. dev.
	1	2	3	4	5	6	7		
Al	4.11	3.69	11.13	2.54	2.53	2.31	2.7	4.14	3.15
C	9.49	12.07	9.74	13.93	13.7	13.39	13.41	12.25	1.89
Cu	39.99	29.29	14.6	29.71	29.9	29.85	30	29.05	7.43
O	14.73	21.94	44.61	18.11	19.47	18.25	18.37	22.21	10.10
Si	0	0.85	0	0	0	0	0	0.12	0.32
Ti	31.68	32.16	19.91	35.71	34.4	36.19	35.52	32.22	5.71

Nevertheless, the detailed element map at the interface shown on the bottom left in Fig 7 shows, that alloying is achieved to some extent across the cross-section by laser powder bed fusion. The distribution at the metal-ceramic interface changes after the samples are subjected to thermal treatments. Titanium deposits at the interface and locally a thin layer is formed. This can be observed in more detail in Fig. 8. The formation of such reaction layers at the interface is well known from active metal brazing processes [18]. An elemental analysis at the marked positions within this interface layer is shown in Table V.

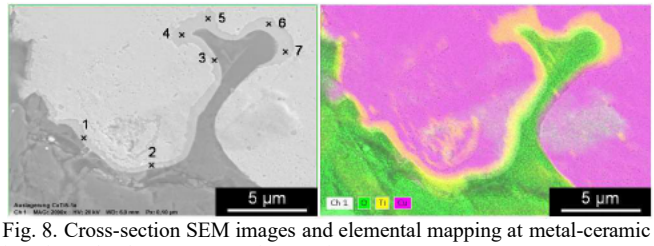

Fig. 8. Cross-section SEM images and elemental mapping at metal-ceramic interface after heat treatment for 60 minutes at 950 °C.

The ratio of detected Cu, Ti and O is an indicator for the phase at the interface, which is likely to be a material system based on Cu, Ti and O with dissolved Al like Cu_2Ti_2O [18] or Cu_3Ti_3O, which is mentioned in [19]. The formation of a reaction layer serves to explain the improved adhesion after thermal treatment.

V. Summary

In this paper a novel approach on manufacturing metal-ceramic-substrates by means of laser powder bed fusion of a powder mixture with titanium as an active element is presented. The adhesion and microstructure of locally fused copper powders with titanium shares of 1 wt.%, 5 wt.% and 10 wt.% was analyzed. Based on a regression model, adhesion optimized parameter values for all powder mixtures are calculated. For 1 wt.% titanium, the adhesion maximizing parameters are parameter range limiting factors, which indicates, that with higher energy input during the laser powder bed fusion process stronger adhesion can be obtained. Further investigations are required to optimize the adhesion for 1 wt.% titanium. For 5 wt.% and 10 wt.% titanium an optimal laser power to maximize the adhesion was identified. Samples with 5 wt.% titanium were then subjected to different heat treatments at varying temperatures and dwell times. The mean adhesion of 18 MPa without heat treatment was improved to 27.8 MPa after a heat treatment at 950 °C for 60 minutes. At 950 °C conchoidal fractures due to thermo-mechanical stresses in the brittle ceramic were observed in cross-section analysis, leading to a more pronounced variation in adhesive strength. Elemental mapping showed locally distributed reaction layers at the metal-ceramic interface after heat treatment at 950 °C for 60 minutes. So these layers seem to increase the adhesion of the metallization.

Acknowledgment

Funded by the Deutsche Forschungsgemeinschaft (DFG, German Research Foundation) – 434962551; 442921285.

References

[1] GERMAN GOVERNMENT. EU-Umweltrat: Nur noch CO2-frei fahren [online]. 2023. https://www.bundesregierung.de/breg-de/schwerpunkte/europa/verbrennermotoren-2058450. Accessed: 6th July 2023.

[2] BERGER, C. Das Erreichen der Klimaziele durch Elektrifizierung [online]. springerprofessional.de. 3rd April 2019, https://www.springerprofessional.de/klimawandel/energie/das-erreichen-der-klimaziele-durch-elektrifizierung/16592690. Accessed: 6th July 2023

[3] JILLEK, W. and G. KELLER. Handbuch der Leiterplattentechnik. Bad Saulgau: Eugen G. Leuze Verlag; Carl Hanser Verlag, 2003. Hanser eLibrary. ISBN 9783874803304

[4] BURGESS, J.F., C.A. NEUGEBAUER and G. FLANAGAN. The Direct Bonding of Metals to Ceramics by the Gas - Metal Eutectic Method. Journal of The Electrochemical Society, 1975, 122(5), S. 688-690. ISSN 1945-7111. doi:10.1149/1.2134293

[5] YOSHINO, Y. and H. OHTSU. Interface Structure and Bond Strength of Copper-Bonded Alumina Substrates. Journal of the American Ceramic Society, 1991, 74(9), S. 2184-2188. ISSN 0002-7820. doi:10.1111/j.1151-2916.1991.tb08281.x

[6] KIM, S.T. and C.H. KIM. Interfacial reaction product and its effect on the strength of copper to alumina eutectic bonding. Journal of Materials Science, 1992, 27(8), S. 2061-2066. ISSN 1573-4803. doi:10.1007/BF01117918

[7] HE, H., R. FU, D. WANG, X. SONG and M. JING. A new method for preparation of direct bonding copper substrate on Al2O3 . Materials Letters, 2007, 61(19-20), S. 4131-4133. ISSN 0167-577X. doi:10.1016/j.matlet.2007.01.036

[8] NICHOLAS, M.G., Hg. Joining of ceramics. London: Chapman and Hall, 1990. Advanced ceramic reviews. ISBN 0412367505

[9] EUSTATHOPOULOS, N. Wettability at High Temperatures. London: Elsevier Science & Technology, 1999. Pergamon Materials Ser. v.Volume 3. ISBN 9780080543789

[10] KELKAR, G.P. and A.H. CARIM. Phase Equilibria in the Ti-AI-O System at 945oC and Analysis of Ti/Al2O3 Reactions. Journal of the American Ceramic Society, 1995, 78(3), S. 572-576. ISSN 1551-2916. doi:10.1111/j.1151-2916.1995.tb08216.x

[11] HONGQI, H., J. ZHIHAO and W. XIAOTIAN. The influence of brazing conditions on joint strength in Al2O3/Al2O3 bonding. Journal of Materials Science, 1994, 29(19), S. 5041-5046. ISSN 1573-4803. doi:10.1007/BF01151094

[12] DIN EN ISO/ASTM 52900. 2022. Additive Fertigung – Grundlagen – Terminologie. Berlin: Beuth Verlag GmbH

[13] SYED-KHAJA, A., D. SCHWARZ and J. FRANKE. Advanced substrate and packaging concepts for compact system integration with additive manufacturing technologies for high temperature applications. In: 2015 IEEE CPMT Symposium Japan (ICSJ).

[14] STOLL, T., KIRSTEIN, M. and FRANKE, J.. A novel approach of copper-ceramic-joints manufactured by selective laser melting. In

Material Technologies and Applications to Optics, Structures, Components, and Sub-Systems IV (Vol. 11101, pp. 53-63). SPIE.

[15] STOLL, T. Laser Powder Bed Fusion von Kupfer auf Aluminiumoxid-Keramiken. 2023.FAU Studien aus dem Maschinenbau Band 420, Erlangen: FAU University Press. ISBN 978-3-96147-632-9

[16] KANG, S.-J.L. Sintering. Densification, Grain Growth, and Microstructure. Oxford: Elsevier Science & Technology, 2005. ISBN 9780080493077.

[17] VALDEZ-NAVA, Z., D. KENFAUI, M.-L. LOCATELLI, L. LAUDEBAT and S. GUILLEMET. Ceramic substrates for high voltage power electronics: past, present and future. In: 2019 IEEE International Workshop on Integrated Power Packaging (IWIPP). Toulouse, France, April 24-26, 2019. Piscataway, NJ: IEEE, 2019, S. 91-96. ISBN 978-1-5386-7610-3

[18] KRITSALIS, P., L. COUDURIER and N. EUSTATHOPOULOS. Contribution to the study of reactive wetting in the CuTi/Al2O3 system. Journal of Materials Science, 1991, 26(12), S. 3400-3408. ISSN 1573-4803. doi:10.1007/BF01124693

[19] HANSEN, M., K. ANDERKO and H.W. SALZBERG. Constitution of Binary Alloys. Journal of The Electrochemical Society, 1958, 105(12), S. 260C. doi: 10.1149/1.2428700